J. Materials, Conc. Struct., Pavements No. 520/V-28, 309-321, August 1995

VERIFICATION OF 3D CONSTITUTIVE MODEL OF CONCRETE IN LINE WITH CAPACITY AND DUCTILITY OF LATERALLY REINFORCED CONCRETE COLUMNS

Tirath Manojya PALLEWATTA[1], Paulus IRAWAN[2] and Koichi MAEKAWA[3]

[1] Dr. of Eng., Former Graduate Student, Dept. of Civil Eng., The University of Tokyo (Hongo 7-3-1, Bunkyo-ku, Tokyo 113, Japan)
[2] Member of JSCE, Ms. of Eng., Graduate Student, Dept. of Civil Eng., The University of Tokyo (Hongo 7-3-1, Bunkyo-ku, Tokyo 113, Japan)
[3] Member of JSCE, Dr. of Eng., Associate Prof., Dept. of Civil Eng., The University of Tokyo (Hongo 7-3-1, Bunkyo-ku, Tokyo 113, Japan)

Three-dimensional elasto-plastic and continuum fracture model for concrete, which had been originally developed with reference to uniform stress field, is verified on structural member level of non-uniformity. This study adopts idealized square concrete cores purely confined by closed square lateral steel ties. The constitutive model is examined in view of confining stress induced from lateral steel to core concrete and enhanced strength and ductility of core concrete at the axial capacity of columns. The verified applicable range of the constitutive model is clarified under practical stress conditions and paths arising in RC column members. The effect of loading rate on the plasticity evolution is also discussed.

Key Words : *constitutive law, confinement, plasticity, fracture, axial strength*

1. INTRODUCTION

Computational mechanics has gained considerable popularity owing to its versatility when we treat structural member behaviors in practice. The attractiveness of this approach is portrayed by wide applicability to different configurations, boundary and loading conditions. Here, one of the most important conditions is the installation of reliable constitutive laws for constituent materials used[2),13)].

Though concrete can not be strictly categorized as a continuum due to micro discontinuities, it can be considered in a finite region on an average basis to be a continuum. Through FEM it is possible to simulate concrete structural behaviors, provided that the constitutive relations incorporated are sound representations of concrete. One of constitutive models for concrete is the combined elasto-plastic and continuum fracture model[9)]. The original model developed for 2D stress states had been enhanced to represent three-dimensional non-linearity in concrete[10)]. This model had been developed and verified under uniform stress fields at the material level under hardening stage arising in the stress-strain curves.

It is indispensable to further examine the applicability of any constitutive model under non-uniform stress fields and realistic stress paths generally encountered in actual reinforced concrete as engineering problems[11)]. For this purpose, the authors applied the constitutive model through FEM to the problem of three-dimensional non-linear behaviors of concrete columns under passive confinement parted by lateral reinforcement in the ascending part of stress-strain relation.

Here indispensable are reliable experimental results which have simple and clear boundary conditions and systematically arranged parameters. On this line, the test program which consists of square concrete columns confined with square perfectly closed ties without longitudinal reinforcement nor cover concrete was adopted[12)]. As the most distinguishing aspect of this test program, 3D lateral tie strains were comprehensively monitored to compute the average confinement parted to the concrete core. Description of the experimental program and related results are discussed elsewhere[12)].

This paper presents the primary verification of the three-dimensional elasto-plastic and continuum

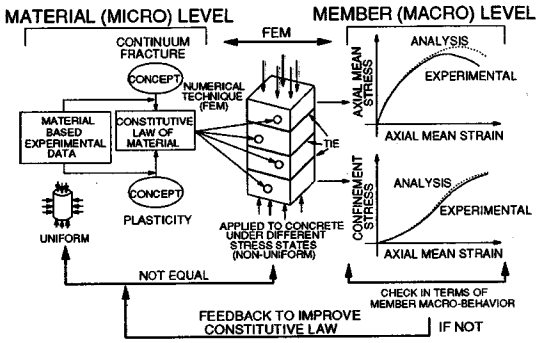

Fig.1 Constitutive law and verification

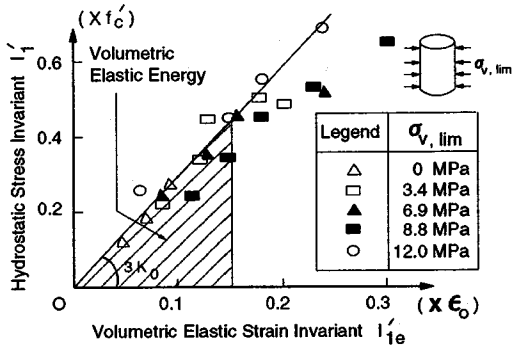

Fig.3 Hydrostatic stress vs. volumetric elasticity

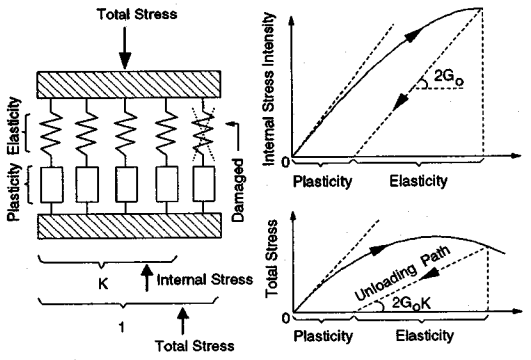

Fig. 2 Elasto-plastic and continuum fracture concept

fracturing model for concrete confinement at member level of stress non-uniformity and the range of applicability of this microscopic approach in the ascending branch of the mean axial stress-strain relation. The concept of this process[11] is again illustrated in **Fig.1**.

2. THREE-DIMENSIONAL ANALYSIS OF STRESS AND DAMAGE

(1) Constitutive law of concrete

The constitutive model of concrete used can be schematically idealized as shown in **Fig.2**. The total stress is identified as the assembly of internal stresses developing over the non-damaged elasto-plastic elements. Here, elastic strain is directly proportional to internal stress intensity applied to active non-damaged elasto-plastic elements. Thus, the elastic strain is chosen to represent the internal stress intensity which governs the plasticity and fracture in the concrete continuum with defects. An index named fracture parameter (K) is introduced to represent the ratio of active volume which can carry internal stress in concrete. The model basically derives from the following four experimental facts simply complied below. Details are discussed in reference 10).

a) Fracture in hydrostatic stress state

It was found that the capacity to store volumetric elastic strain energy is not affected by the level of 3D confinement nor by the level of damage induced in concrete[10]. It means that the entire volume of concrete is active with respect to the volumetric elasticity. **Fig.3** shows that regardless of the level of applied confinement, the relationship between the hydrostatic stress invariant (I_1) and the volumetric elastic strain invariant as (I_{1e}) remains constant, mathematically described as[4],

$$I_1 = 3K_0 I_{1e} \qquad (1)$$

$$I_1 \equiv \sigma_{kk}/3 \quad I_{1e} \equiv \varepsilon_{ekk}/3$$

where, K_0 is the volumetric elastic constant and σ_{ij} and ε_{eij} are total stresses and elastic strain tensors, respectively.

b) Fracture in shear

The level of damage caused by shear in concrete influences the capacity of concrete to store shear elastic strain energy[10]. The continuum damage represented by the fracture parameter K is evolved by the internal shear stress intensity, while retarded by volumetric confinement. Plot of the stress deviator invariant against the elastic strain deviator invariant in **Fig.4** shows that the relationship between two is affected by the level of confinement.

To represent the response of damaged concrete in shear, the model adopts the relationship between total stress deviator invariant (J_2) and elastic strain deviator invariant (J_{2e}) as,

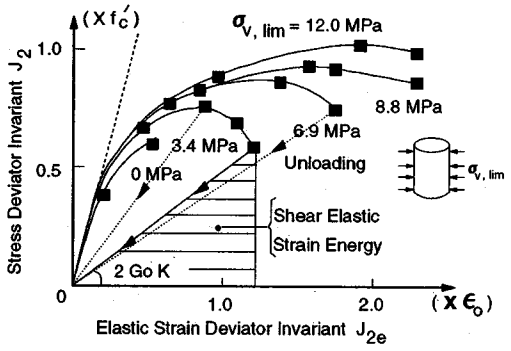

Fig.4 Deviator stress vs. strain invariant

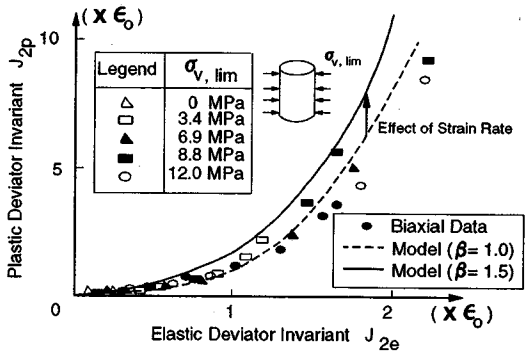

Fig.5 Plastic progress in shear mode

$$J_2 = 2G_0\, K(F)\, J_{2e} \qquad (2)$$

$$J_2 \equiv \sqrt{\sigma_{ij}\cdot\sigma_{ij}/2} \quad J_{2e} \equiv \sqrt{\varepsilon_{eij}\cdot\varepsilon_{eij}/2}$$

where, F is a damage measure function of J_{2e}, J_{3e}, and I_{1e}, and G_0 is the initial elastic shear stiffness.

Since the level of fracture is path dependent, the maximum of the value, F_{max} experienced in the past loading history of concrete is taken as the value for F in Eq.(2). If the updated value of F is smaller than any previous value, the fracture condition is assumed to be stable with no progress of damage. With higher confinement, propagation of micro defects is restrained. It implies that higher confinement results in a larger fraction of concrete domain contributing in shear mode resistance at a given shear elastic strain.

It was found that when the fracture parameter K becomes smaller than 0.25, strain localization in compression is induced in concrete. Here, strain field is no longer uniform and absolute strain is size-dependent. Thus, this value is tentatively identified as applicability limit of the model.

c) Plasticity in shear

Plasticity in deviatoric shear denoted by J_{2p} is advanced by the internal shear stress intensity represented by J_{2e}. However, it was found that deviatoric plasticity is not influenced by the volumetric confinement as shown in **Fig.5**. This effect is represented by plastic hardening function H as[10],

$$J_{2p} = H(J_{2e\max}) \qquad (3)$$

$$J_{2p} \equiv \int \frac{e_{ij}\, d\varepsilon_{pij}}{2\, J_{2e}}$$

where, $J_{2e\ max}$ is the maximum of J_{2e} during past loading histories, e_{ij} is elastic strain deviator tensor, and ε_{pij} is plastic strain tensor. When the updated value is lower than any previous value, evolution of plasticity is assumed to be unchanged. Based on uniformly confined experiments, plastic hardening function, (H=$H(J_{2e})$) has been proposed for normal concrete.

Here, it must be reminded that the plastic evolution function was formulated with reference to the short-term loading test of concrete solids[10]. When stress rate arising in real structures would differ from the condition on which the function H was based, we have to take into account the time-dependent plasticity in the verification process. In fact, it was reported by Okamura et al.[11] under 2D states that plastic evolution law of concrete has to be modified in terms of real loading rate produced in target structures, and the following simple correction factor is used for cyclic analysis of RC plate as,

$$J_{2p} = \beta \cdot H(J_{2e}) \qquad (4)$$

where, β=1.5 for laboratory structural experiments.

The authors hereafter discuss the difference of loading rate between the material based test condition and the structural reality with respect to the correction factor. The use of correction factor (β) to take into account the effect of loading rate is in accordance to previous studies about the effect of strain rate to the strength and ductility of plain and confined concrete. It was found that higher strain rate will increase the strength and ductility of plain as well as confined concrete[1),3),5)]. It took only several minutes to apply the load to the specimen from zero to the peak in deriving the model. On the other hand, several hours were needed in case of real structures tested in laboratories. This difference in the loading time affects the plastic evolution of

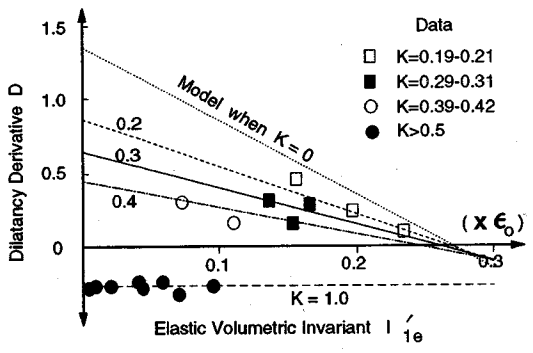

Fig.6 Dilatancy Derivative

concrete and the correction factor is adopted to take into account this effect.

Since the time dependent fracturing and damage evolution are reported to be comparatively less affected by the stress rate[11], time dependent fracturing will not be discussed in this study.

d) Plasticity in volume

The volumetric plastic strain (I_{1p}) associated with shear plasticity (J_{2p}) is significantly affected by the magnitude of confinement[10]. This non-linearity named *shear dilatancy* is indicated by the dilatancy derivative (D) given in Eq.(5) and Eq.(6).

$$d I_{1p} = D(I_{1e}, K) d J_{2p} \tag{5}$$

$$d I_{1p} = \tfrac{1}{3} d\varepsilon_{pkk} \tag{6}$$

Based on experimental data, the *dilatancy derivative* ($D=D(I_{1e}, K)$) has been formulated[10] and shown in **Fig.6**. Increase in confinement causes this expansion or dilatancy to be reduced.

Since the progress of volumetric plastic strain is gradual according to the level of damage in the concrete and confinement applied to it, continuous function of dilatancy derivative (D) is utilized as,

$$D = D_0 K^2 + D_1 (1-K)^2 \tag{7}$$

The effect of Poisson's ratio and confinement is taken into account in D_o and D_1, respectively[10].

As stated above, the effect of confinement is classified into continuum fracture and plasticity in terms of volumetric and deviatoric aspects. The above four relations and equations are the core of the three-dimensional continuum fracture and plasticity constitutive law. By solving the above proposed simultaneous equations, we have the incremental constitutive equations in terms of total stress and strains as,

$$d\{\sigma\} = [M]([I] + [L])^{-1} d\{\varepsilon\} \tag{8}$$

where, $[M]$ and $[L]$ represent the fracture and plasticity matrices, respectively[10].

Owing to the combination of plasticity and fracturing formula, the constitutive model covers strain hardening and softening, continuously and consistently. When higher confinement would be created, evolution of fracturing in shear is restrained. It coherently makes the overall behavior of concrete more plastic as it is.

As stated above, the softening behavior can be mathematically dealt with by the model proposed. But, at this moment, the authors regard the post peak softening as being out of applicability. Material functions and coefficients are formulated as element size-independency for simplicity. It means that the model cannot be applied in general to strain softening range in which the apparent constitutive relation is much size-dependent. Then, the authors firstly concentrate on the strain hardening 3D behaviors up to the peak strength of size-independency even though the model can originally cover the softening zone.

(2) Model of Reinforcement

Steel bars used as lateral reinforcement were modeled under two idealizations of truss members only capable of resisting axial loads and beam members having flexural and shear stiffness incorporated.

With the first idealization of steel as truss model which is simpler in analytical implementation, 3D isoparametric element having just axial stiffness and translational degree of freedom at nodes was implemented. Since the rotational degree of freedom is not incorporated, bending moment and shear force developing along the element cannot be idealized.

For the second idealization of steel, Timoshenko beam element[14] was selected. In this element, a plane section initially normal to the mid-surface remains plane but not necessarily normal to it. This condition allows transverse shear deformation. Both translational displacement and rotational fields are interpolated along the finite element. Then, the flexural stiffness can be taken into account for larger sections of steel bars. As the shear energy term is involved, reduced integration scheme proposed by Zienkiewicz[14] is adopted for avoiding "shear

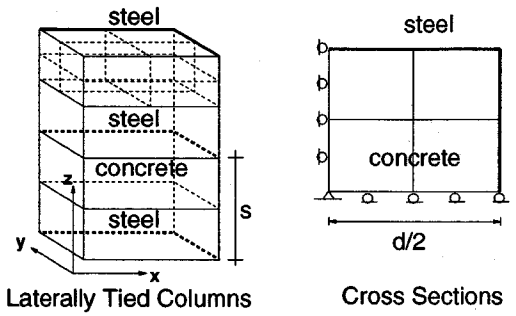

Fig.7 Finite element discretization

locking". Stress-strain relation assumed for steel is the elastic perfect plastic model.

(3) Finite element idealization

Square members considered for this analysis has axial symmetry which enables only one fourth of the member in the lateral direction to be discretized as finite elements. In the longitudinal direction, two layers of concrete isoparametric elements with 20 nodes are applied which divide the half tie spacing into two. To account for the non-uniformity in the lateral direction four solid concrete elements per layer are adopted as shown in **Fig.7**. This discretization was decided by conducting preliminary check for mesh size convergence in the hardening stage of columns concerned.

Loading is accomplished by applying forced axial displacement to the top surface of the concrete with bottom surface maintained as a fixed boundary. Computation was conducted in the ascending part of the concrete axial stress-strain behavior in consideration of the mesh sensitivity for compression softening.

One of core information adopted for verification is mean axial stress-strain relation of columns. This relation is a reflection of local plasticity and damage of concrete in the light of overall response of members. The other one is the mean confining stress defined as,

$$\sigma_v \equiv \frac{1}{V_c}\int_{V_c}\sigma_c\, dv, \quad \sigma_c \equiv \frac{\sigma_{c,xx}+\sigma_{c,yy}}{2} \tag{9}$$

which represents the degree of confinement actually induced from lateral reinforcing bars and is also closely associated with the plastic dilatancy and continuum fracturing model of concrete. Here, $\sigma_{c,ij}$ is the stress tensor of concrete and *Vc* is the volume of the analysis domain.

The confinement effectiveness of lateral reinforcement is quantified by confinement effectiveness index denoted by α[6),7),12)] which is the ratio of actually induced spatial average confining stress at the peak strength of confined core to the potential confinement capacity ($\sigma_{v,lim}$) when all lateral steel attains yield as,

$$\alpha = \frac{\sigma_v}{\sigma_{v,\mathrm{lim}}}, \qquad \sigma_{v,\mathrm{lim}} = -\frac{1}{2}\, p\, f_y \tag{10}$$

where, p denotes the volumetric ratio of lateral reinforcement to that of the concrete core, and f_y is the yield strength of steel.

Confinement effectiveness is reflected in increase in the axial compressive capacity of confined concrete core and the related ductility. For verifying micro-mechanical approach on member level, both confinement effectiveness and capacity enhancement have to be focused.

3. FLEXURAL EFFECT OF LATERAL REINFORCING BARS

In RC structural analysis it is generally assumed that reinforcing steel only carries axial stress as truss or chord members. This hypothesis represents lateral reinforcement member with finite axial stiffness and infinitely small flexural one which would apply confinement only at corners of square concrete core.

Practically used lateral reinforcing bars however have a finite flexural stiffness which could contribute to the confinement mechanism. Neglecting this effect might result in underestimating confinement efficiency by steel. In implementation of 3D micro mechanical constitutive models of concrete for evaluating confinement phenomena, it is necessary to identify the most appropriate modeling of lateral steel. For this purpose steel modeling as truss and beam elements have to be investigated.

To differentiate between two idealizations, results of a special experiment creating the confinement stress conditions that would be developed in only corner confined concrete was used[12)]. Here, contact between concrete and lateral steel was removed by deformable spacing material, except at corners, resulting in stress transfer only at four corners of the square core. This condition creates only axial forces

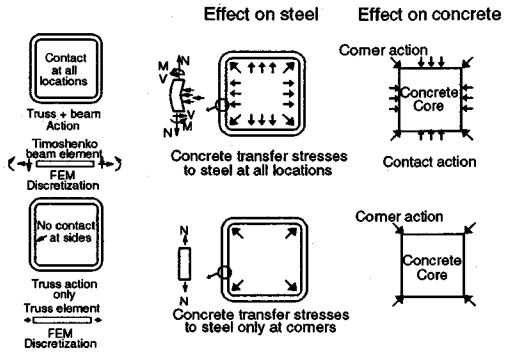

Fig.8 Confinement mechanisms by lateral ties

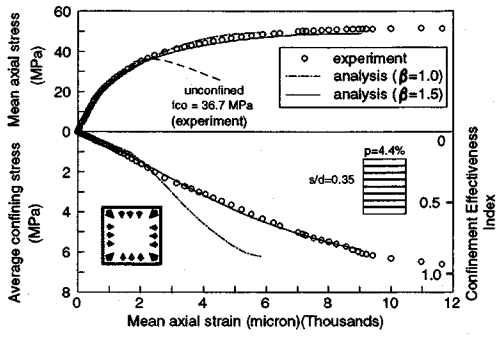

Fig.10 Normally confined column
(Timoshenko's beam element is used in analysis)

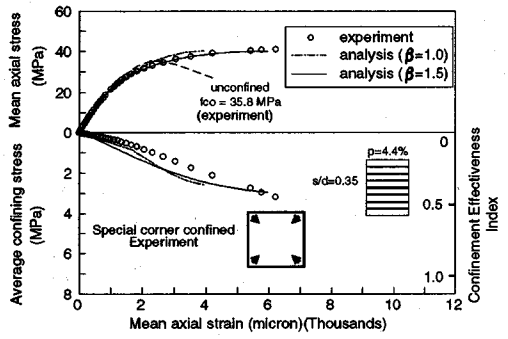

Fig.9 Corner confined column
(Truss element is used in analysis)

in ties. A normally confined column with the same confinement parameters and the contact between steel and concrete occurred at all locations was also used for comparison. The confinement mechanisms for the two experiments are illustrated in **Fig.8**. To simulate the experimental results of axial mean stress-strain and confinement through FEM analysis, steel was modeled as truss and Timoshenko's beam members for the two cases, respectively. Since heavily reinforced columns possess larger diameter bars having unavoidable shear stiffness, Timoshenko's beam theory which allows shear deformation is realistic and thought to be appropriate as a lateral tie model.

The observed and computed axial peak strengths of confined core given in **Fig.9** for the corner action case are seen to match very closely along the stress-stain paths. Especially, accuracy of the member strength has much to do with the constitutive model for continuum fracturing.

On the other hand, computed deformability and ductility are dominantly associated with the model for plastic evolution. The mean axial strain at the peak load is seen to be higher for experiment as compared with analysis with the original plastic evolution law. This may be attributed to the strain rate used in developing the microscopic concrete model (10-100μ/sec), which was higher than that used in experiment (0.1-1μ/sec). **Fig.9** includes analytical result based on factored plastic evolution (β=1.5) as stated in Eq.(4). The strength gain computed is not affected but the ductility prediction is much improved.

These results show that the special experiment is a reasonable physical representation of the truss idealization of steel in the FEM simulation.

Similar results on the companion normal specimen is shown in **Fig.10**. In this case the experimentally developed peak strength, strain at capacity as well as induced average confining stress at the peak, are much higher than the special experiment. This structural enhancement can be directly attributed to the effect of contact or beam action of lateral ties. Comparison with the FEM analysis data based on beam elements show that, peak strength as well as the spatial average confining stress developed at the peak strength are very closely matched by the FEM results.

Strain at the capacity is underestimated when the original plastic evolution law is used, a trend similar to what was identified through **Fig.10**. This observation can be explained again on the grounds of effect of strain rate used in the experimental development of the microscopic concrete model. In fact, when the same factored plasticity (β=1.5) is applied, overall ductility is also improved.

As further clarification of the two idealization methods, confinement stress uniformity at the critical section of the core is compared. Critical section governing the peak strength of the core is the

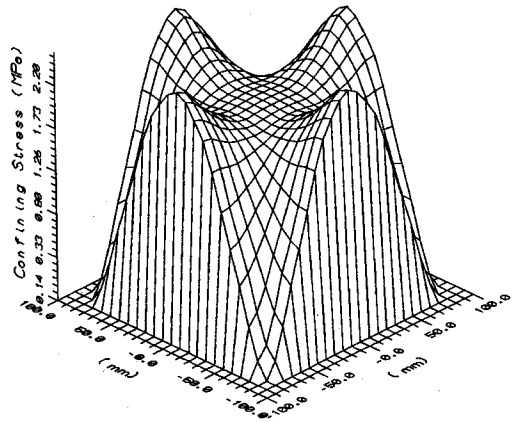

Fig. 11 Confining stress at critical section (steel idealized as truss elements)

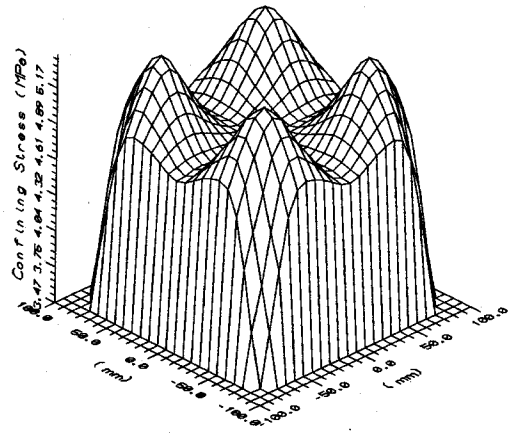

Fig.12 Confining stress at critical section (steel idealized as beam elements)

midway point between two discretely placed lateral ties. Results of FEM analytical method is used to compute the distribution of local lateral confining stress σ_c defined as the in-plane lateral stress invariant given by Eq.(9).

Computed lateral confining stress distribution under truss idealized case[7] is shown in three-dimensional diagram of **Fig.11**. Similar diagram for the case of beam idealized analysis is depicted in **Fig.12**. At four corners, in-plane normal stresses in x- and y-directions exactly get zero because concrete at the corner of the critical section between ties is exposed to free surfaces on which no external force is applied in all directions. Then, the confining stress defined by Eq.(9) becomes zero at four corners. It is seen from these diagrams that the confinement stress distribution across the cross section of the core is more uniform in the case of beam element analysis. Furthermore, the absolute values of the confining stresses are seen to be much higher in this case as compared to truss element based analysis. It means more confinement is applied to the core concrete if steel is modeled as beam element than truss element. These observations further indicate the appropriateness of modeling the confining reinforcement as beam elements.

From these experimental and analytical comparisons, it is clear that for simulation of general confinement phenomena, lateral steel should be modeled as beam elements rather than analytically simpler truss elements in case of the heavily reinforced columns of lateral steel. Even if the lateral reinforcement would be light, larger diameter bars with greater bending stiffness are used for confinement agent in the case of larger spacing. Therefore, it is required to use beam idealization regardless of the amount of lateral ties specified.

4. CONFINEMENT EFFECTIVENESS - CAPACITY OF CORE CONCRETE -

The idealized experimental investigation was conducted on a wide range of lateral reinforcement content and spacing[12]. Content of lateral reinforcement is quantified in terms of volumetric lateral reinforcement ratio (p). Spacing of lateral reinforcement normalized by the minimum core dimension (s/d) is used for geometry factor of lateral ties. The confined core is assumed to be bound by centerlines of peripheral lateral reinforcement.

Since the flexural and shear stiffness of lateral ties is found to be dominant for confinement as discussed in the previous chapter, the following FEM analysis is based on steel idealized as beam elements. Comparison of FEM simulation results pertaining to confinement level and strength of confined core at its peak strength, with results of experimental program[12] is given in **Table 1**. Here, the maximum available confining stress denoted by $\sigma_{v,lim}$ in Eq.(10) is reached if all lateral steel attains yield condition at the core peak given by $\frac{1}{2}pf_y$.

(1) Axial Mean Stress and Confinement Stress

The relation of most interest in regard to the macro behavior of confined concrete columns is the mean axial stress-strain variation. It is the objective of the microscopic approach to correctly predict this non-linearity up to the peak strength of concrete.

Table 1 FEM analysis results at peak strength for confined columns in the experimental program[12)]

Designation and Comments	Spac. ratio (s/d)	Average confining stress (σ_v)			Strength of core concrete (MPa)		
					Uncon fined (f_{co})	Confined (f_{cc})	
		Max. avail able	Exp.	FEM		Exp.	FEM
C16-075 high r/f	0.41	9.49	7.64	6.58	36.9	59.5	50.7
D19-104 high r/f	0.58	9.24	7.20	5.43	35.6	53.5	46.8
O19x2-232 high r/f	1.20	8.49	1.72	1.60	35.2	39.0	38.2
A09-042 medium r/f	0.22	5.40	5.06	4.71	35.6	46.3	46.4
H13-094 medium r/f	0.51	4.99	3.67	3.69	35.6	43.9	43.3
I16-150 medium r/f	0.83	4.56	2.11	2.77	35.6	42.6	41.1
J19-225 medium r/f	1.26	4.38	1.07	1.76	35.6	39.9	38.8
M09-090 low r/f	0.48	2.52	1.80	2.12	35.2	40.3	40.0
N13-192 low r/f	1.04	2.45	0.64	1.41	35.2	37.7	38.0
P09-043 small core	0.31	7.13	6.38	6.03	38.0	53.0	51.2
S25-119 big core	0.32	6.61	5.63	5.54	37.3	51.3	49.5
T13-065 size effect flex. effect	0.35	7.22	6.56	5.84	36.7	51.8	49.0
U13-065-C corner action	0.35	7.22	3.15	2.92	35.8	41.1	39.9
V16-075-LS high r/f low f_{co}	0.41	9.12	7.18	5.22	27.5	46.4	38.6

Note) Compression is specified positive in this table.

Through this approach, this curve is cumulatively generated based on elasticity, plasticity and continuum damage.

To understand the tendency of analytical method as compared with experimental results, three pairs of specimens are considered in the following discussions. Since the yield strength of lateral steel for this study is kept nearly constant, the reinforcement ratio is a direct indicator of potential confinement capacity.

The mean axial stress-strain relations, both experimental and computed, for nearly same (p≅3%) lateral reinforcement ratio with different spacing ratios are studied first. This medium reinforcement ratio was selected to present the standard conditions used in the experimental program. Experimental and analytical comparisons are given through **Fig.13** for closely tie spaced column and through **Fig.14** for more widely tie spaced one. Confinement effectiveness index is also placed on the same axis

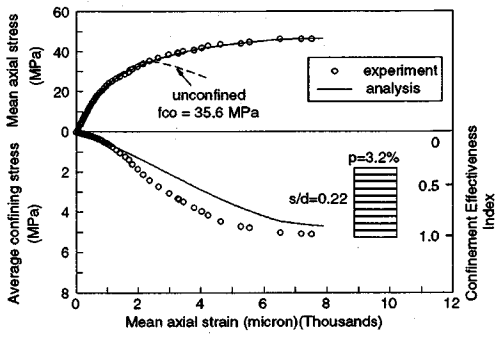

Fig.13 Mean axial stress-strain and confinement (p=3.2%, s/d=0.22)

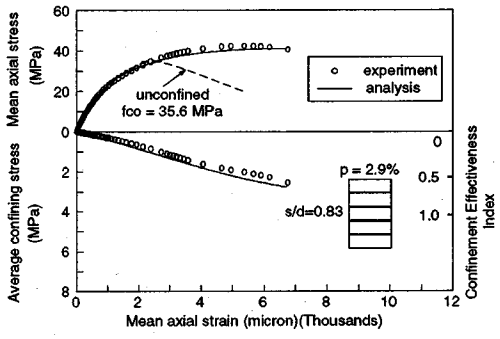

Fig.14 Mean axial stress-strain and confinement (p=2.9%, s/d=0.83)

with the spatial average confining stress for indication of the level of confinement.

It is seen that for both columns FEM prediction on the peak strength fairly matches. For the column with lower spacing ratio, computed mean axial stress-strain path matches quite well with the experimental observation. The induced average confining stress path is predicted fairly well by analysis in the beginning of loading and also close to the peak including the confinement produced at the peak strength of the core.

In the case of higher spacing, mean axial stress-strain path as well as confining stress path is very closely predicted. Peak strength of core concrete and the strain at peak strength are also predicted very well.

The computed stress-strain relation is compared with experimentally observed for low (p=1.5%) and medium (p=2.8%) reinforcement ratio with spacing ratio above unity. The spacing ratios are s/d=1.04 and s/d=1.26, respectively. Physical meaning of this spacing condition is that the ties are arranged with a

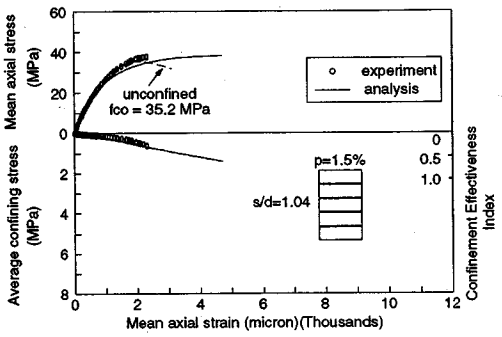

Fig.15 Mean axial stress-strain and confinement (p=1.5%, s/d=1.04)

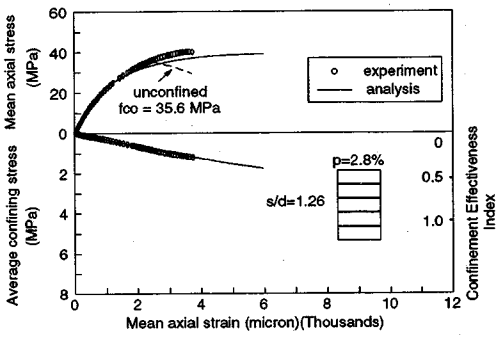

Fig.17 Mean axial stress-strain and confinement (p=2.8%, s/d=1.26)

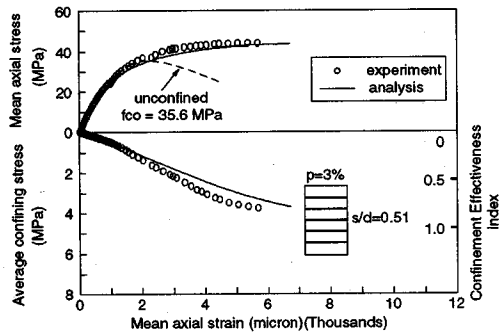

Fig.16 Mean axial stress-strain and confinement (p=3.0%, s/d=0.51)

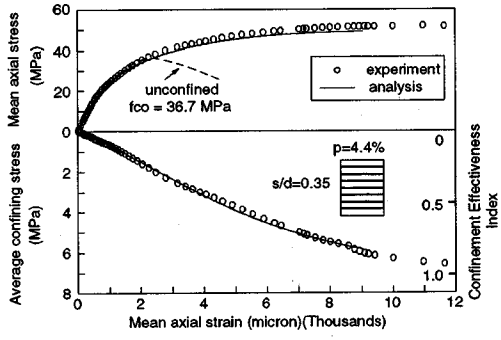

Fig.18 Mean axial stress-strain and confinement (p=4.4%, s/d=0.35)

spacing more than the core size. The mean axial stress-strain as well as induced average confining stress versus mean axial strain of the core is given in **Fig.15** and **Fig.17**, respectively. For the lower reinforcement ratio, strength is matched quite well.

It is observed that the experimental mean axial strain at peak strength is lower than the analytical prediction by about 50%. This discrepancy might be attributed to the instability which occurs to the core concrete close to the peak, since the spacing is quite large. Experimental induced average confining stress is also about 50% lower than the predictions by analysis at the peak strength of the core. However, the absolute values of average confining stress are small.

For the medium reinforcement case presented by **Fig.17**, the peak strength prediction is satisfactory. Still overprediction of the strain at peak strength is seen, similar to the previous case in **Fig.15**. Further it is observed that the induced confinement variation is predicted well until the peak strength of the experiment. Confinement at the peak strength of the core is overpredicted by the analysis.

A typical set of curves for practically applicable lower spacing ratio are considered as the third pair. The mean axial stress-strain curve and induced average confining stress against mean axial strain curves are plotted in **Fig.16** for volumetric reinforcement ratio of 3.0% with a spacing ratio of 0.51. The peak strength and axial stress-strain paths are quite well matched for this case. The analytical induced confining stress is also seen to vary quite closely with the experimental curve. A deviation is observed near the peak strength.

For the reinforcement ratio on the higher side (p=4.4%), and spacing ratio of 0.35, comparison curves are shown in **Fig.18**. Axial peak strength as well as the axial mean stress-strain curves for the analytical result and experimental observations is closely matched. However, little underprediction of the experimental value is seen for the strain at peak strength of the core. The induced confining stress is

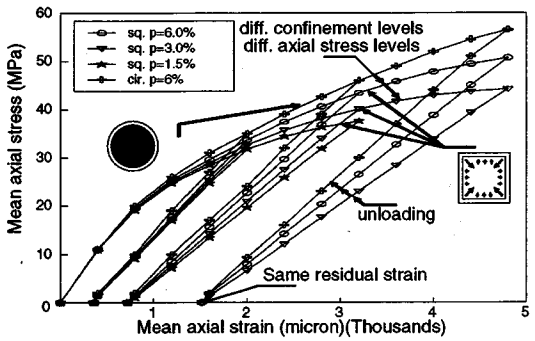

Fig.19 Analytical response of confined cores under cyclic loading

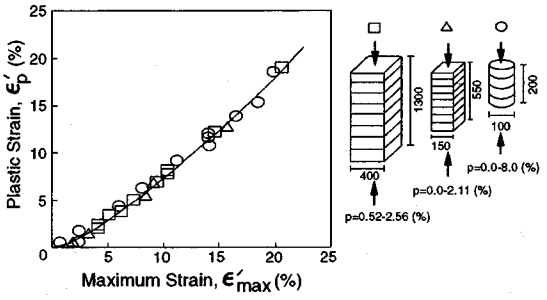

Fig.20 Experimentally obtained residual strains under different confinement levels and sections[8)]

seen to match very closely with the experimental value at the peak strength of the core.

It is observed that from the six comparisons above, the peak strength is quite well predicted while the strains at peak strength of the core are varying. This could be attributed to the different strain rates used in developing the material relations of the micro model with respect to experiments compared as stated before. It is noted from these curves that generally, for lower spacing ratios, (i.e., closely spaced ties) the predictions of peak strength as well as confining stress level at peak strength are matched quite well by the computational method. For higher spacing conditions, the analytical method predicted the peak strengths quite closely.

However, the analysis exhibits a general tendency of slightly overpredicting the confining stress level at the peak strength of the core for large spacing. In the case of small reinforcement ratio with closer arrangement of ties, both strength gain and confinement effectiveness were fairly predicted. This behavior will be discussed with other combination of lateral reinforcement ratio and spacing in the later section again.

(2) Cyclic loading

As a further discussion of the characteristics of microscopic constitutive law based approach, unloading and residual deformations are considered. **Fig.19** shows axial stress-strain relations of three cases of square concrete cores and a circular core with different confinement levels. These four levels were generated with the same sized lateral tie placed at different spacing, resulting in varying lateral reinforcement ratios. For this analysis beam idealization was adopted for square cores and truss idealization was used for circular core since the bending moment never be introduced owing to the point symmetry around the center of section. In the simulations unloading was commenced at three discrete levels of axial mean strain.

It is noteworthy that the residual axial strains are not influenced by the different axial stress levels at the start of unloading. Experimental verification for this phenomenon is obtained from Ref. 8). Here, laterally confined square as well as circular concrete columns has been subjected to cyclic axial compressive loading. At the conclusion of each cycle, the residual axial strain is plotted against the maximum axial strain to which the column had been subjected, in **Fig.20**. It is seen that the above relation is not influenced by the confining arrangement or shape signifying different levels of confinement. It can be said with reference to this figure that the residual plastic deformation under axial loading is not affected by the level of confinement as formulated in Eq.(4).

This phenomenon incorporated into the constitutive law by the relation indicated in **Fig.5** in section 2 is verified by above observations on member level applicability. It is seen from this figure that the relationship between plastic deviatoric strain and elastic deviatoric strain is not influenced by the confinement level.

Another advantage of confinement is identified by this discussion, which allows confined concrete to attain higher axial stress levels without generating excess residual plastic deformations. The practical significance is realized when confined members are subjected to repeated overloading, but resulting in lower permanent deformations indicating better serviceability condition.

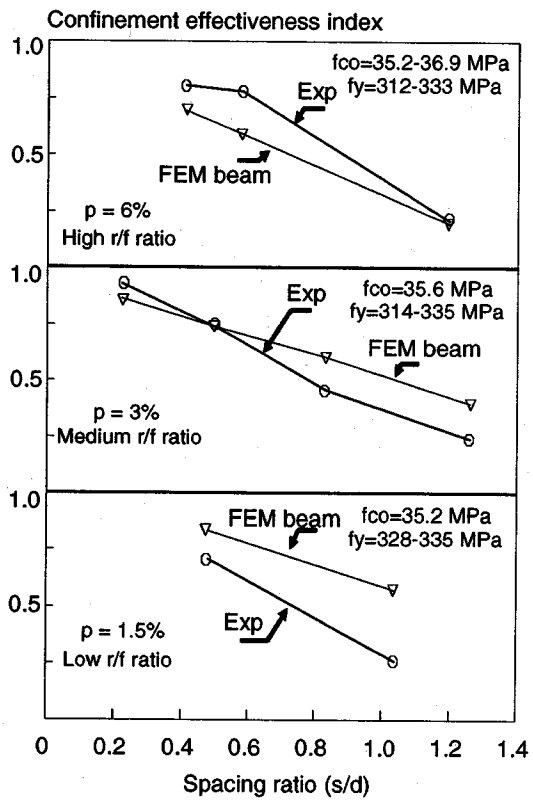

Fig.21 Confinement effectiveness index against tie spacing and reinforcement ratio

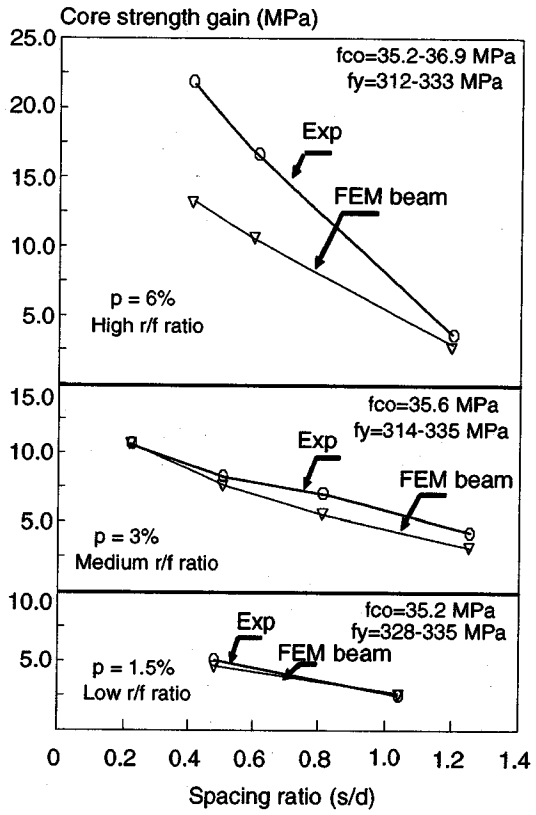

Fig.22 Core strength gain against tie spacing and reinforcement ratio

(3) Spacing and Amount of Lateral Reinforcement

Spacing and the amount of lateral reinforcement which are most influential in the effect of confinement at the peak strength of the confined concrete core are addressed as further discussion of the verification of the micro-mechanical approach. For this purpose three ranges of reinforcement content were selected. Reinforcement content given as the volumetric reinforcement ratio is a direct indicator of the potential confinement capacity since steel yield strengths used were in a very close range as mentioned earlier.

Confinement effectiveness index obtained from experiments as well as computed with the FEM analysis are compared for different spacing under the three lateral reinforcement contents in **Fig.21**. Here the FEM analysis results with lateral steel idealized as beam elements are seen to be close with the experimentally observed for closely spaced conditions (s/d<0.6), in all three ranges of reinforcement content. For higher spacing a general tendency of overprediction by FEM analysis is observed.

As further verification **Fig.22** shows the core strength gains due to confinement at the peak strength by experiment and analysis, in the same ranges as discussed above. It is observed that for lower to medium reinforcement content (p=1.5% - p=3%) the strength gains are predicted quite well for all spacing. For the higher reinforcement content (p=6%) a general tendency of under-prediction of the strength gain is shown by the analytical method.

In consideration of both confinement effectiveness index and strength gain at the peak strength of confined concrete core, it is seen that the FEM analytical method is successful in simulating the behavior when the lateral reinforcement is closely placed (s/d < 0.6) and the content less than 4.4% by reinforcement ratio. Reinforcement content of 4.4% with lower spacing was also seen to produce good comparison in both confinement effectiveness index and strength gain as indicated through **Fig.22**. This

verified range is of much practical importance since it represents the mostly adopted lateral reinforcement configurations. Higher spacings are not suitable due to the low confinement effectiveness and higher lateral reinforcement ratios are not practicable in generally confined columns with longitudinal reinforcement.

5. CONCLUSIONS

This study was aimed at verifying the non-linear three-dimensional elasto-plastic and continuum fracture model on laterally reinforced concrete member level through FEM analytical method. For the verification purpose, idealized experimental results on axially loaded confined columns reported elsewhere were used.

Based on the results of special experiment which applied confinement only at corners with contact between tie arms and concrete eliminated, the truss idealization of the lateral steel in the FEM method was verified. Through this verification it was identified that steel should be modeled as beam members capable of resisting flexure and shear, in order to simulate actual confined concrete cores. This is in contrast to the common analytical assumption of modeling reinforcement as truss members. Comparisons were carried out between typical experimental results and analysis based on beam idealization of reinforcing steel. Mean axial stress-strain relations until the peak strength of confined concrete were compared in conjunction with spatial average confining stress. Special attention was paid to the peak strength level due to its significance.

FEM simulations of axial cyclic loading of confined concrete indicated that the confinement level does not influence the residual strain when the maximum induced strain experienced in the loading paths be the same. This was verified by experimental results of cyclically loaded concrete cores.

From the comparisons it is concluded that the behavioral trends observed in experiments were closely simulated by the analytical method throughout the lateral reinforcement detailing ranges. On a quantitative basis, the 3-Dimensional FEM method is identified to be effective in simulating the confinement effectiveness and strength enhancement, when smaller spacings ($s/d < 0.6$) are adopted with medium to low reinforcement ratios ($p<4.4\%$). These ranges are significant since the verified applicability of the analytical method represents the practical application domain.

In the case where much heavy reinforcement be arranged ($p>4.4\%$), computation based on the constitutive model brings about underestimation of the strength of confined cores. This is thought to be rooted in the insufficient accuracy of the fracture evolution model in the constitutive law under higher confinement conditions as being pointed out in the reference 10). For further improvement of the constitutive model, the plasticity and fracturing evolution rules under much higher confinement conditions should be promoted.

ACKNOWLEDGMENT: This study was financially supported by Grant-in-Aid for scientific research No.04555114 from The Ministry of Education in 1995.

REFERENCES

1) Ahmad, S.H., and Shah, S.P.: Behavior of Hoop Confined Concrete under High Strain Rates, *ACI Journal*, Vol. 82, pp. 634-647, 1985.

2) Bangash, M.Y.H.: *Concrete and Concrete Structures: Numerical Modeling and Applications*, Elsevier Applied Science, London, 1989.

3) Chen, W.F.: *Plasticity in Reinforced Concrete*, McGraw Hill Book Co., New York, 1982.

4) Chen, W.F., and Saleeb, A.F.: *Constitutive Equations for Engineering Materials, Vol. 1 : Elasticity and Modeling*, John Wiley & Sons, New York, 1982.

5) Dilger, W.H., Koch, R., and Kowalczyk, R.: Ductility of Plain and Confined Concrete under Different Strain Rates, *ACI Journal*, Vol. 81, pp. 73-82, 1984.

6) Irawan, P., and Maekawa, K.: Strength and Damage Analysis of Concrete Confined by Steel Casing, *Journal of Materials, Concrete Structures and Pavements*, JSCE, Vol.20, No.472, pp.97-106, 1993.

7) Irawan, P., and Maekawa, K.: Three-Dimensional Analysis on Strength and Deformation of Concrete Confined by Lateral Reinforcement, *Journal of Materials, Concrete Structures and Pavements*, JSCE, Vol.20, No.472, pp.107-118, 1993.

8) Maekawa, K., Song, C., and Irie, M.: Unified Concept for Compressive Characteristics of Concrete.-From 3D Confinement to Pre-cracking, *JCI Colloquium*, Analytical Studies on Shear Design of Reinforced Concrete Structures, pp. 31-38, 1989.

9) Maekawa, K., and Okamura, H.: The Deformational Behavior and Constitutive Equations for Concrete Using Elasto-plastic and Fracture Model, *Journal of the Faculty of Engineering*, The University of Tokyo (B), 37(2), pp. 253-328, 1983.

10) Maekawa, K., Takemura, J. Irawan, P., and Irie, M.: Triaxial Elasto-Plastic and Continuum Fracture Model for Concrete, *Concrete Library*, JSCE, No. 22, pp. 131-161, 1993.

11) Okamura, H., and Maekawa, K.: *Nonlinear Analysis and Constitutive Models of Reinforced Concrete*, Gihodo-Syuppan, Tokyo, 1991.

12) Pallewatta, T. M., Irawan, P. nd Maekawa, K.: Effectiveness of Laterally Arranged Reinforcement on the Confinement of Core Concrete, (to be published).

13) Task Committee on Finite Element Analysis of Reinforced Concrete Structures of the Structural Division Committee on Concrete and Masonry Structures, *Finite Element Analysis of Reinforced Concrete*, ASCE, New York, 1982.

14) Zienkiewicz, O. C.: *The Finite Element Method*, McGraw-Hill, 1977.

(Received November 25, 1994)

横補強されたコンクリート柱の耐力と靭性に立脚した3次元コンクリート構成則の検証

Tirath Manoja PALLEWATTA, Paulus IRAWAN and Koichi MAEKAWA

本研究は，均一な応力・ひずみ状態の元で得られた実験から導かれたコンクリートの3次元弾塑性破壊型構成式を，柱部材中の不均一な応力状態において解析的に検証を行ったものである．検証の対象とした部材は，完全併合型の横補強筋により拘束される矩形断面コアコンクリートであり，中心軸圧縮状態を想定した．拘束効果に伴う軸耐力および圧縮靭性の向上，拘束鉄筋応力とコアコンクリートに導入される拘束応力について，実験結果と3次元構成則を用いた有限要素解析結果との比較を行った．その結果，弾塑性破壊型構成式の精度と適用範囲が検証され，さらに載荷速度の影響が主として塑性変形の進行に関して無視できないことが確認された．

Mr.SOIL Ver.3.5 for Windows

It's NEW!

業界すべてのエンジニアへ
優れた機能を抜群のコストパフォーマンスで。

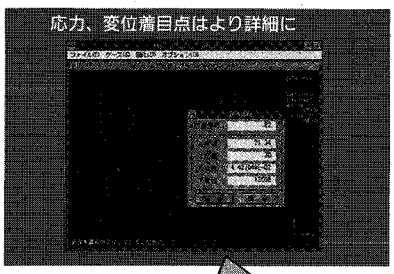

Step1
オートメッシュで簡単に
メッシュデータ作成

Step4
さらに詳細検討へ

Real Easy! Real Speedy!

Mr.SOILは地盤の応力、変形特性、土木構造物との相互作用を総合的に解析可能な強力なFEM解析ツールです。

販売実績：400本超
（国内外含：'95.3現在）

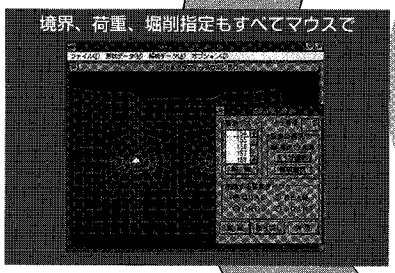

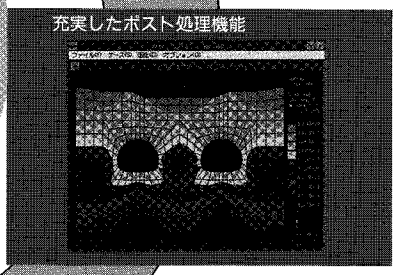

Step2
高速、高精度ソルバーへ

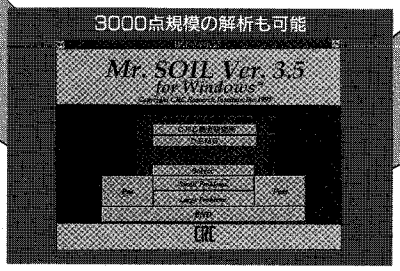

Step3
各種ポスト処理へ

●動作環境
CPU：80386以上（推奨 80486以上）
Windows 3.1
メモリ640Kbyte+7Mbyte以上
ハードディスク10Mbyte以上

●価格　¥980,000ー（税別）
旧バージョンをご使用中のお客様は、バージョンアップ価格を、また、2本目以降マルチライセンス価格も設定しておりますのでお問い合わせ下さい。

*Windowsは米国マイクロソフト社の商標です。

■詳細資料または、ご検討のためのDemo Systemをご希望のお客様は、下記の問い合わせ先までご連絡下さい。

土木CAE業界をリードするCRC土木ソフトウェアラインアップ

地下水解析：3次元地下水解析…SEEPAGE-3D
広域地下水変動解析…UNISSF(V-2)、PC/
地質解析：3次元地質解析…GEORAMA
地盤解析：2、3次元地盤解析…Mr.SOIL
連成解析：土・水の連成（逆）解析…UNICOUP
岩盤・地盤解析：個別要素法…UDEC、3DEC
＊これらのソフトを使用しての受託解析業務も行って

日本技術開発株資料室

8011063

●開発／発売元

株式会社CRC総合研究所
I学システム営業部／担当：村中
市中央区久太郎町4-1-3
241-4121　FAX：06-241-4136
I部／建設エンジニアリング部
都江東区南砂2-7-5
5634-5789　FAX：03-5634-7337

土と水の連成逆解析プログラム

未来設計企業 CRC

UNICOUP

応力解析と浸透解析がドッキングした!

軟弱地盤の解析に!

海洋開発・埋立

盛土・掘削

出力項目

- 各節点での変位、各要素での応力
- 各節点での全水頭・圧力水頭 他
- 豊富な図化処理
  変位図、変位ベクトル図、応力ベクトル図、応力コンター図、安全率コンター図、水頭コンター図、圧力水頭コンター図

プログラムの特長

- 応力と地下水の流れをカップルさせた問題が解析可能です。(圧密含む)
- 地下水の流れは飽和・不飽和域を対象としています。
- 多段掘削・盛土や降雨等が扱えます。
- 梁や連結要素も扱え実用的です。
- 経時観測記録(変位・水位)があれば、非線形最小二乗法に基づき変形係数や透水係数が逆解析できます。(順解析、逆解析がスイッチにて選択可能です。)
- 弾性・非線形弾性・弾塑性・弾粘塑性を示す地盤が扱えます。
  非線形弾性(電中研式、ダンカン・チャンの双曲線モデル)
  弾塑性(ドラッカー・プラガー、モール・クーロン、カムクレイモデル、ハードニング、ソフトニング)
  弾粘塑性(関口・太田モデル)

応力増分コンター(Δσ V)
(10日後)

変位ベクトル図 (40日後)

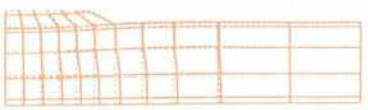

盛土(40日)後の地盤の変形

盛土(40日)後の地下水の流れと水頭コンターおよび自由水面

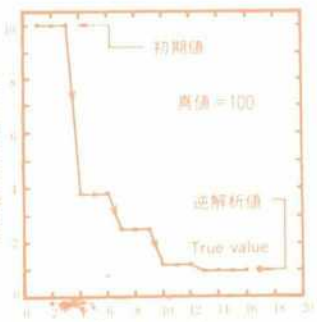

ヤング率と繰り返し回数の関係

逆解析によるパラメータの推定

この製品は、情報処理振興事業協会の委託を受けて開発したものです。
通商産業省 特別認可法人
IPA 情報処理振興事業協会

株式会社CRC総合研究所 西日本支社

〒105 東京都港区芝公園三丁目1番38号
TEL.(03)3437-2301

問合せ先
〒541 大阪市中央区久太郎町4丁目1-3
(06) 241-4121 営業担当:岩 崎
(03)3665-9741 本社窓口:菅 原